Methyleneoxirane–Cyclopropanone and Related Rearrangements in C_3H_4O Cation Radicals and Neutral Molecules. A Quest for the Oxyallyl Intermediate

Frantisek Turecek,*,† Donald E. Drinkwater, and Fred W. McLafferty*

Contribution from the Department of Chemistry, Baker Laboratory, Cornell University, Ithaca, New York 14853-1301. *Received December 10, 1990*

Abstract: The formation, relative stabilities, isomerizations, and dissociations of several C_3H_4O cation radicals and neutral molecules have been investigated by neutralization–reionization mass spectrometry (NRMS) and ab initio calculations (MP4/6-31G*). The methyleneoxirane (**1**$^{\bullet+}$) and $^{\bullet}CH_2CH_2CO^+$ (**4**$^{\bullet+}$) ions were found experimentally as stable, noninterconverting species, consistent with the results of ab initio calculations. Upon collisionally activated dissociation (CAD), prior to losing the ring methylene group, **1**$^{\bullet+}$ undergoes partial degenerate isomerization via the oxyallyl ion, $CH_2\text{–}C(O^{\bullet})CH_2^+$ (**3**$^{\bullet+}$). The activation barriers for the **3**$^{\bullet+}$ → **1**$^{\bullet+}$ and **1**$^{\bullet+}$ → **3**$^{\bullet+}$ isomerizations were calculated as 8 and 105 kJ mol^{-1}, respectively. The cyclopropanone cation radical **2**$^{\bullet+}$, is unstable, representing a transition state for the degenerate isomerization of $^{\bullet}CH_2CH_2CO^+$ (**4**$^{\bullet+}$), while the distonic ion $CH_2{=}C^+{-}OCH_2^{\bullet}$ (**7**$^{\bullet+}$) and the ion–molecule complex $CH_2{=}CH_2^{\bullet+}\cdots OC$ (**14**$^{\bullet+}$) are stable. Neutral methyleneoxirane (**1**) is found to be a stable molecule that does not undergo extensive degenerate isomerization upon its formation from the ion **1**$^{\bullet+}$. The biradical $^{\bullet}CH_2CH_2CO^{\bullet}$ produced by neutralization of **4**$^{\bullet+}$ is unstable, dissociating to C_2H_4 and CO in <1 μs with a large kinetic energy release. NRMS is superior to CAD in distinguishing $C_3H_4O^{\bullet+}$ isomers.

The electrocyclic ring opening in methyleneoxirane (**1**) leading to cyclopropanone (**2**) has been studied intensively for over two decades following Hoffmann's extended-Hückel-theory calculations[1] that suggested the oxyallyl intermediate **3** (Scheme I). More recent semiempirical[2] and ab initio[3] calculations have indicated that **3** should be substantially less stable than both **1** and **2**, setting its 0 K potential energy 204 kJ mol^{-1} above that of **2**,[3b] consistent with thermochemical estimates.[4] The question of whether **3** represents a stable equilibrium structure or a transition state (saddle point) has been a matter of agrument.[3a,5] The most recent multiple-configuration SCF calculations have found both the singlet ($^1A_1$) and the triplet ($^3B_2$) states of **3** to be stable equilibrium structures; however, the activation barriers to ring closures in **3** have not been studied.[5]

These predictions present a challenge for experimentalists in both the preparation and identification of oxyallyl. The existence of alkyl-substituted oxyallyl intermediates has been inferred from trapping experiments that employed aldehydes and dienes for [3 + 2] or [3 + 4] cycloadditions, respectively.[6] However, attempts at preparation of **3** have been unsuccessful so far, in part due to the extreme reactivity of its ring-closed isomers **1** and **2** that undergo fast thermally induced polymerization in the condensed phase.[7,8] On photolysis **2** dissociates to ethylene and carbon monoxide.[8] According to ab initio calculations[9] the C-1–C-2 ring opening in **2** should proceed via a triplet biradical intermediate $^{\bullet}CH_2CH_2CO^{\bullet}$ (**4**) whose existence, however, has remained speculative because of lack of experimental evidence.

A preliminary report of this study describes the preparation of **1** in the gas phase[10] by charge-transfer neutralization of the corresponding cation radical **1**$^{\bullet+}$, utilizing neutralization–reionization mass spectrometry (NRMS).[11] NRMS has been implemented to generate a variety of other marginally stable species, e.g, hypervalent radicals ($D_3O^{\bullet}$,[12] ND_4,[13] $H_2Cl^{\bullet}$ [14]), ylides ($^-CH_2ClH^+$ [15] and $^-CH_2{}^+SHOH$[16]), and biradicals ($^{\bullet}CH_2OCH_2^{\bullet}$, $^{\bullet}CH_2CH_2O^{\bullet}$).[17] The availability of **1**$^{\bullet+}$ and **1** opened a route to studying the oxyallyl rearrangement of both cation radicals and neutral molecules. That of gaseous cation radicals is of special interest, as these often exhibit cyclizations and cycloreversions whose mechanisms and energetics are entirely different from those of their neutral closed-shell counterparts.[18] In this paper the unimolecular and collisionally activated dissociations (CAD) of several isomeric C_3H_4O cation radical and neutral species related to **3** and **4** are examined. The relative stabilities and isomerization barriers of these species are addressed by ab initio calculations.

Scheme I

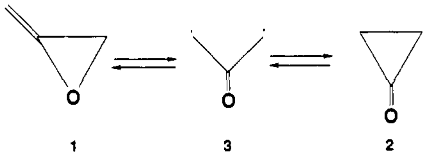

---

† Present address: Department of Chemistry, University of Washington, Seattle, WA 98195.

(1) Hoffmann, R. *J. Am. Chem. Soc.* **1968**, *90*, 1475–1485.

(2) (a) Liberles, A.; Kang, S.; Greenberg, A. *J. Org. Chem.* **1973**, *38*, 1922–1924. (b) Liberles, A.; Greenberg, A.; Lesk, A. *J. Am. Chem. Soc.* **1972**, *94*, 8685–8688. (c) Pochan, J. M.; Baldwin, J. E.; Flygare, W. H.; *J. Am. Chem. Soc.* **1969**, *91*, 1896–1898. (d) Olsen, J. F.; Kang, S.; Burnelle, J. *J. Mol. Struct.* **1971**, *9*, 305–313. (e) Bodor, N.; Dewar, M. J. S.; Harget, A.; Haselbach, E. *J. Am. Chem. Soc.* **1970**, *92*, 3854–3859.

(3) (a) Schaad, L. J.; Hess, B. A.; Jr.; Zahradník, R. *J. Org. Chem.* **1981**, *46*, 1909–1911. (b) Ortiz, J. V. *J. Org. Chem.* **1983**, *48*, 4744–4749. (c) Lahti, P. M.; Rossi, A. R.; Berson, J. A. *J. Am. Chem. Soc.* **1985**, *107*, 2273–2280.

(4) Liebman, J. F.; Greenberg, A. *J. Org. Chem.* **1974**, *39*, 123–130.

(5) (a) Osamura, Y.; Borden, W. T.; Morokuma, K. *J. Am. Chem. Soc.* **1984**, *106*, 5112–5115. (b) Coolidge, M. B.; Yamashita, K.; Morokuma, K.; Borden, W. T. *J. Am. Chem. Soc.* **1990**, *112*, 1751–1754. (c) Ichimura, A. S.; Lahti, P.; Matlin, A. R. *J. Am. Chem. Soc.* **1990**, *112*, 2868–2875.

(6) (a) Camp, R. L.; Greene, F. D. *J. Am. Chem. Soc.* **1968**, *90*, 7349. (b) Turro, N. J.; Edelson, S. S.; Williams, J. R.; Darling, T. R.; Hammond, W. B. *J. Am. Chem. Soc.* **1969**, *91*, 2283–2292. (c) Turro, N. J. *Acc. Chem. Res.* **1969**, *2*, 25–32. (d) Noyori, R.; Yokoyama, K.; Hayakawa, Y. *J. Am. Chem. Soc.* **1973**, *95*, 2722–2723. (e) Chan, T. H.; Li, M. P.; Mychajlowskij, W.; Harpp, D. N. *Tetrahedron Lett.* **1974**, 3511–3514.

(7) For reviews see: (a) Marvell, E. N. *Thermal Electrocyclic Reactions*; Academic Press: New York, 1980; pp 55–66. (b) Stang, P. J. In *The Chemistry of Ethers, Crown Ethers, Hydroxyl Groups and Their Sulphur Analogues, Supplement E, Part 2*; Patai, S., Ed.; Wiley: Chichester, 1980; Chapter 19, pp 859–879. (c) L'abbé, G. *Angew. Chem.* **1980**, *92*, 277–290. (d) Wasserman, H. H.; Berdahl, D. R.; Lu, T.-J. In *The Chemistry of the Cyclopropyl Group, Part 2*; Rappoport, Z., Ed.; Wiley: Chichester, 1987; Chapter 23, pp 1455–1530.

(8) Rodriguez, H. J.; Chang, J.-C.; Thomas, T. F. *J. Am. Chem. Soc.* **1976**, *98*, 2027–2034.

(9) Yamabe, S.; Minato, T.; Osamura, Y. *J. Am. Chem. Soc.* **1979**, *101*, 4525–4531.

(10) Turecek, F.; Drinkwater, D. E.; McLafferty, F. W. *J. Am. Chem. Soc.* **1990**, *112*, 5892–5893.

(11) (a) Gellene, G. I.; Porter, R. F. *Acc. Chem. Res.* **1983**, *16*, 200–207. (b) Wesdemiotis, C.; McLafferty, F. W. *Chem. Rev.* **1987**, *87*, 485–500. (c) Terlouw, J. K.; Schwarz, H. *Angew. Chem., Int. Ed. Engl.* **1987**, *26*, 805–815. (d) Holmes, J. L. *Adv. Mass Spectrom.* **1989**, *11*, 53. (e) Terlouw, J. K. *Adv. Mass Spectrom.* **1989**, *11*, 984. (f) Holmes, J. L. *Mass Spectrom. Rev.* **1989**, *8*, 513–539. (g) McLafferty, F. W. *Science* **1990**, *247*, 925–929.

0002-7863/91/1513-5950$02.50/0

Experimental Section

Measurements were made with a tandem mass spectrometer described previously consisting of a modified Hitachi RMH-2 double-focusing mass spectrometer as the first mass analyzer (MS-I), a special collision region furnished with three collision cells, an electrostatic analyzer (ESA-II) as MS-II, and a second magnet as MS-III.[19] For $^+NR^+$ mass spectra the ions produced at 70 eV electron energy and accelerated to 9.9 keV are selected by MS-I and allowed to undergo charge-exchange neutralization with Hg vapor at 70% transmittance in the first collision cell.[20] The remaining ions are deflected electrostatically, and the resulting fast neutrals are reionized with oxygen at 50% transmittance in the second collision cell.[21] For $^+NCR^+$ mass spectra, the selected neutrals exiting from the first collision cell undergo collisions with helium (50% transmittance) in the second collision cell; the ions formed are deflected electrostatically, and the remaining neutrals reionized by collisions with oxygen (50% transmittance) in the third collision cell. For charge reversal ($^+NR^-$) experiments, benzene (25% transmittance) was used as a single target gas in the second collision cell. For CA/CAD experiments, the ions were collided with helium in the first field-free region, selected by MS-I, and allowed to collide with oxygen (50% transmittance) in the third collision cell, and the CAD products were analyzed by ESA-II.

2,3-Epoxypropyl 4-Nitrobenzene (5). A solution of 4-nitrobenzoyl chloride (Fluka, 3.7 g, 20 mmol) in ether (50 mL) was added at 0 °C to a stirred solution of freshly distilled 2,3-epoxypropanol (Aldrich, 3.0 g, 40 mmol) in 10% aqueous NaOH (20 mL). TLC analysis (silica gel, chloroform) 1 h after the addition showed that the reaction was completed; the ethereal layer was separated and dried over sodium sulfate, and the solvent was evaporated. The solid residue was recrystallized from acetone–water to give 3.66 g (82%) of **5**, mp 41–42 °C. ^1H NMR (Varian XL-200, 200.057 MHz, $CDCl_3$, 20 °C): 8.26 (2 H), 8.21 (2 H), AB (J = 9.2 Hz); 4.71 (1 H), 4.15 (1 H), 3.33 (1 H), ABX ($|J_{AB}|$ = 12.2 Hz, J_{AX} = 2.8 Hz, J_{BX} = 6.5 Hz); 2.90 (1 H), 2.72 (1 H), A′B′X ($|J_{A'B'}|$ = 4.8 Hz, $J_{A'X}$ = 4.4 Hz, $J_{B'X}$ = 2.7 Hz). MS (m/z, rel intensity) 223 ($M^{\bullet+}$, 0.5), 222 (0.3), 167 (2), 150 (100), 134 (10), 120 (6), 104 (24), 103 (6), 92 (10), 76 (17), 75 (10), 65 (2), 56 (17), 50 (13).

2,3-Epoxypropyl-*1,1*-d_2 4-Nitrobenzoate (5a). To a stirred solution of 2-propen-1-ol-*1,1*-d_2[22] (1.28 g, 21 mmol) in 10% aqueous NaOH (25 mL) was added at 0 °C a solution of 4-nitrobenzoyl chloride (11.66 g, 63 mmol) in ether (45 mL). The mixture was stirred for 1 h, and then 10 mL of 10% NaOH was added and the stirring continued for 30 min. The ethereal layer was separated and dried with sodium sulfate, and the solvent was evaporated in vacuo. The crude semisolid ester (3.6 g, 81%) was dissolved in CH_2Cl_2 (50 mL) and treated with 3-chloroperoxybenzoic acid (85%, Aldrich, 10 g) for 72 h at 0 °C. The separated 3-chloroperoxybenzoic acid was filtered off and washed with CH_2Cl_2, the solution was washed three times with 10% Na_2CO_3 and dried with Na_2SO_4, and the solvent was evaporated in vacuo. The solid residue was recrystallized from acetone–water to give 2.8 g (72%) of **5a**, mp 41–42 °C. ^1H NMR ($CDCl_3$, 20°C): 8.34 (2 H), 8.23 (2 H), AB (J_{AB} = 9.3 Hz); 3.37 (m, 1 H), 2.95 (dd, 1 H), 2.76 (dd, 1 H). MS (m/z, rel intensity): 225 ($M^{\bullet+}$, 0.5), 150 (100), 120 (15), 104 (42), 103 (20), 92 (24), 76 (47), 75 (33), 74 (6), 58 (54), 57 (12), 50 (49). 4-Methylene-1,3-dioxolane (**6**) was prepared according to a literature procedure.[23] MS (m/z, rel intensity) 86 ($M^{\bullet+}$, 13), 85 (100), 84 (11), 69 (2), 59 (4), 58 (23), 57 (29), 56 (13), 55 (14), 44 (17), 43 (6), 42 (4), 41 (2), 39 (4), 30 (9), 29 (4), 28 (19), 27 (32), 26 (11), 25 (6).

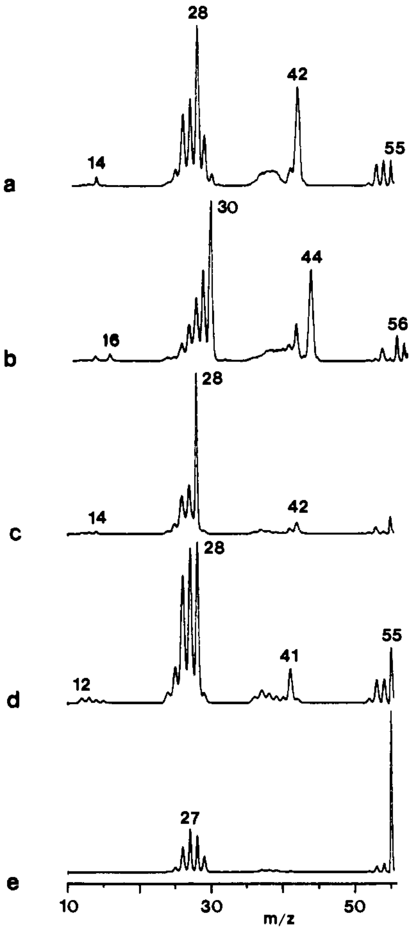

Figure 1. Collisionally activated dissociation spectra (O_2, 50% transmittance) of (a) $1^{\bullet+}$, (b) $1a^{\bullet+}$, (c) $4^{\bullet+}$, (d) $9^{\bullet+}$, and (e) $13^{\bullet+}$.

Scheme II

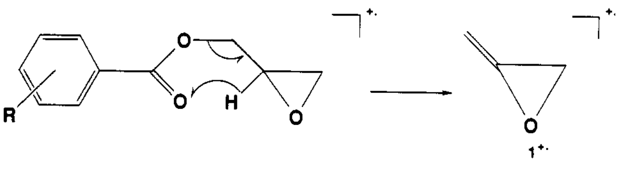

R	relative intensity (%)
4-CH_3	0.1
3-CH_3	0.3
H	2.9
4-F	5.6
3-Br	8.6
4-CN	9.3
4-NO_2	16.9

Calculations. Standard ab initio molecular orbital calculations were carried out with use of the GAUSSIAN 88 program.[24] Geometry optimizations were performed at the HF/6-31G* level. Harmonic vibrational frequencies, also calculated at the HF/6-31G* level, were used both to

---

(12) Gellene, G. I.; Porter, R. F. *J. Chem. Phys.* **1984**, *81*, 5570–5576.

(13) Gellene, G. I.; Porter, R. F. *Int. J. Mass Spectrom. Ion Proc.* **1985**, *64*, 55–66.

(14) Wesdemiotis, C.; Feng, R.; McLafferty, F. W. *J. Am. Chem. Soc.* **1986**, *108*, 5656–5657.

(15) (a) Danis, P. O.; Wesdemiotis, C.; McLafferty, F. W. *J. Am. Chem. Soc.* **1983**, *105*, 7454–7456. (b) Terlouw, J. K.; Kieskamp, W. M.; Mommers, A. A.; Burgers, P. C. *Int. J. Mass. Spectrom. Ion Proc.* **1985**, *64*, 245–250. (c) Wesdemiotis, C.; Feng, R.; Danis, P. Q.; Williams, E. R.; McLafferty, F. W. *J. Am. Chem. Soc.* **1986**, *108*, 5847–5853.

(16) Turecek, F.; Drinkwater, D. E.; McLafferty, F. W. *J. Am. Chem. Soc.* **1989**, *111*, 7696–7701.

(17) Wesdemiotis, C.; Leyh, B.; Fura, A.; McLafferty, F. W. *J. Am. Chem. Soc.* **1990**, *112*, 8655–8660.

(18) (a) Haselbach, E.; Bally, T.; Lanyiova, Z. *Helv. Chim. Acta* **1979**, *62*, 577–582. (b) Haselbach, E.; Bally, T.; Lanyiova, Z.; Baertschi, P. *Helv. Chim. Acta* **1979**, *62*, 583–592. (c) Aebischer, J. N.; Bally, T.; Roth, K.; Haselbach, E.; Gerson, F.; Qin, X.-Z. *J. Am. Chem. Soc.* **1989**, *111*, 7909–7914. (d) Heinrich, N.; Koch, W.; Morrow, J. C.; Schwarz, H. *J. Am. Chem. Soc.* **1988**, *110*, 6332–6336. (e) Pancir, J.; Turecek, F. *Chem. Phys.* **1984**, *87*, 223–232. (f) Groenewold, G. S.; Gross, M. L. *J. Am. Chem. Soc.* **1984**, *106*, 6569–6575. (g) Turecek, F.; Pancir, J.; Stahl, D.; Gaumann, T. *Org. Mass Spectrom.* **1985**, *20*, 360–367. (h) Turecek, F.; Pancir, J.; Stahl, D.; Gaumann, T. *Org. Mass Spectrom.* **1987**, *22*, 145–153. For reviews see: (i) Turecek, F.; Hanus, V. *Mass Spectrom. Rev.* **1984**, *3*, 85–152. (j) Dass, C. *Mass Spectrom. Rev.* **1989**, *9*, 1–36.

(19) McLafferty, F. W.; Todd, P. J.; McGilvery, D. C.; Baldwin, M. A. *J. Am. Chem. Soc.* **1980**, *102*, 3360–3363. Feng, R.; Wesdemiotis, C.; Baldwin, M. A.; McLafferty, F. W. *Int. J. Mass Spectrom. Ion Proc.* **1988**, *86*, 95–107.

(20) Danis, P. O.; Feng, R.; McLafferty, F. W. *Anal. Chem.* **1986**, *58*, 348–354.

(21) Danis, P. O.; Feng, R.; McLafferty, F. W. *Anal. Chem.* **1986**, *58*, 355–358.

(22) Bartlett, P. D.; Tate, F. A. *J. Am. Chem. Soc.* **1953**, *75*, 91–93.

(23) Mattay, J.; Thünker, W.; Scharf, H.-D. *Synthesis* **1983**, 208–210.

(24) Frisch, M. J.; Head-Gordon, M.; Schlegel, H. B.; Raghavachari, K.; Binkley, J. S.; Gonzalez, C.; DeFrees, D. J.; Fox, D. J.; Whiteside, R. A.; Seeger, R.; Melius, C. F.; Baker, J.; Martin, R. L.; Kahn, L. R.; Stewart, J. J. P.; Fluder, E. M.; Topiol, S.; Pople, J. A. GAUSSIAN 88; Gaussian Inc.: Pittsburgh, PA.

Scheme III

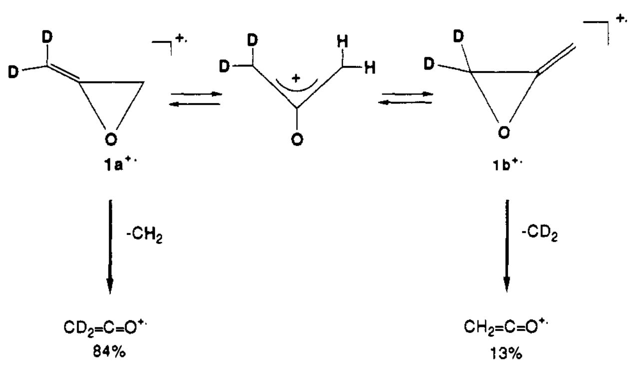

Scheme IV

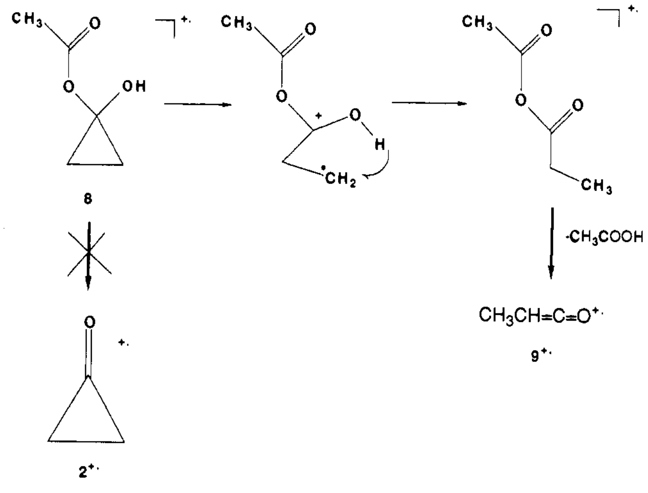

characterize stationary points on the surface as minima (all frequencies real, representing equilibrium structures) or first-order saddle points (one imaginary frequency, representing transition structures) and (after scaling by 0.9) to calculate zero-point vibrational contributions to relative energies. The calculated frequencies are available as supplementary material. Improved relative energies were obtained through calculations on the HF/6-31G* optimized geometries with use of Møller–Plesset perturbation theory[25] terminated at second (MP2), third (MP3), and fourth (MP4) orders. Our best theoretical relative energies (those in the text) correspond to 0 K MP4/6-31G* values, together with the zero-point vibrational corrections. The scaled harmonic frequencies were also used to calculate the 298 K heat contents and estimate standard heats of formation.

Results and Discussion

Cation Radicals. The generation of neutral molecules by NRMS depends on the unequivocal preparation and selection of the corresponding ion counterparts whose structures can be assigned or elucidated through CAD spectra.[26] The methyleneoxirane ion ($\mathbf{1}^{\bullet+}$) was prepared by carboxylic acid eliminations from a variety of 2,3-epoxypropyl esters (acetate, benzoate, 4-F, 3-Br, 4-CN, and 4-NO_2 benzoates, Scheme II).[10] Owing to the relatively high ionization energy of neutral **1** (9.81–9.86 eV),[10] the formation of $\mathbf{1}^{\bullet+}$ is suppressed in dissociations of precursors that can produce complementary fragments of lower ionization energies, e.g. 1-(phenylsulfinyl)-2,3-epoxypropane forming ionized C_6H_5SOH (IE = 8.45 eV),[27] 5,6-epoxyhexan-2-one forming ionized $CH_2{=}C(OH)CH_3$ (IE = 8.61 eV),[28] or spiro[norborn-2-en-5,2′-oxirane] forming ionized cyclopentadiene (IE = 8.57 eV).[29]

Unimolecular dissociation of metastable $\mathbf{1}^{\bullet+}$ (lifetime 13–16 μs) gives rise to $C_3H_3O^+$ (30%) and $C_2H_4^{\bullet+}$ (100%). These dissociations have also been observed for other $C_3H_4O^{\bullet+}$ isomers,[30] and probably involve common transition states that lead to lowest energy products.[31] The CAD mass spectrum of $\mathbf{1}^{\bullet+}$ is distinctly different from those of other $C_3H_4O^{\bullet+}$ isomers (Figure 1a) in that it shows structurally significant fragments at m/z 42 ($C_2H_2O^{\bullet+}$, loss of CH_2), 30 ($CH_2O^{\bullet+}$), and 14 ($CH_2^{\bullet+}$). The formation upon CAD of $C_2H_2O^{\bullet+}$ in competition with $C_2H_4^{\bullet+}$ is remarkable in view of the large difference in the threshold energies for these dissociations (ΔE = 314 kJ mol^{-1})[31] which should favor $C_2H_4^{\bullet+}$. This indicates that there is a significant energy barrier separating $\mathbf{1}^{\bullet+}$ from those $C_3H_4O^{\bullet+}$ isomers that can dissociate directly to $C_2H_4^{\bullet+}$ and CO.

The loss of methylene from $\mathbf{1}^{\bullet+}$ was further investigated with the labeled derivative $\mathbf{1a}^{\bullet+}$ prepared from 2,3-epoxypropyl-*1,1*-d_2 4-nitrobenzoate (**5a**). The CAD spectrum (40% transmittance) of $\mathbf{1a}^{\bullet+}$ (Figure 1b) shows a predominant m/z 44 fragment due to loss of the ring methylene group (84 ± 1%), and a smaller CD_2 loss (m/z 42, 13 ± 1%).[33] The loss of CHD due to hydrogen exchange between the methylene groups is insignificant (2.8 ± 0.3%). The loss of the ring CH_2 group is compatible with the formation of the most stable $CH_2{=}C{=}O^{\bullet+}$ ion (Scheme III); other $C_2H_2O^{\bullet+}$ isomers are substantially less stable.[34] This loss can be explained by a rupture of the C–C bond in $\mathbf{1}^{\bullet+}$ forming the distonic isomer $CH_2{=}C^+{-}O{-}CH_2^{\bullet}$ ($\mathbf{7}^{\bullet+}$); although we have no experimental evidence for its existence, ab initio calculations suggest it to be a stable species (see below). The minor loss of CD_2 requires O–CH_2 oxirane ring opening prior to or during the dissociation; a direct elimination of the exocyclic methylene would produce an unstable oxiranylidene ion.[34] The CD_2 loss could occur directly from $\mathbf{3}^{\bullet+}$ or after degenerate isomerization (or even with isomerization of $\mathbf{2}^{\bullet+}$).

These isomerizations of $\mathbf{1}^{\bullet+}$ were further examined by their collisional activation (CA) to increase the fraction of *nondissociating* $\mathbf{1a}^{\bullet+}$ ions of high internal energy. These excited ions could presumably undergo degenerate $\mathbf{1a}^{\bullet+} \rightleftarrows \mathbf{1b}^{\bullet+}$ isomerization (Scheme III), exchanging the CH_2 and CD_2 groups and leading eventually to an increased loss of CD_2 upon CAD. However, activation by collisions with helium at 40 or 20% transmittance (multiple collision conditions)[35] ca. 10 μs prior to CAD showed $[C_2D_2O^{\bullet+}]:[C_2HDO^{\bullet+}]:[C_2H_2O^{\bullet+}]$ = 85:3:12 and 86:3:11, respectively, unchanged within experimental error from the simple CAD values above. By contrast, the values did depend on the number of collisions, and thus on the energy transferred, in the collisionally activated *dissociation* of the $\mathbf{1a}^{\bullet+}$ ions. Upon decreasing the average number of collisions the $[C_2H_2O^{\bullet+}]/[C_2D_2O^{\bullet+}]$ abundance ratio increased, showing 0.15, 0.40, and 0.55[36] at 40, 80, and 95% transmittance, respectively. This

---

[25] (a) Møller, C.; Plesset, M. S. *Phys. Rev.* **1934**, *46*, 618–622. (b) Pople, J. A.; Binkley, J. S.; Seeger, R. *Int. J. Quantum Chem. Symp.* **1976**, *10*, 1–19.

[26] (a) McLafferty, F. W.; Bente, F. P., III; Kornfeld, R.; Tsai, S.-C.; Howe, I. *J. Am. Chem. Soc.* **1973**, *95*, 2120–2129. (b) McLafferty, F. W.; Kornfeld, R.; Haddon, W. F.; Levsen, K.; Sakai, I.; Bente, P. F., III; Tsai, S.-C.; Schuddemage, H. D. R. *J. Am. Chem. Soc.* **1973**, *95*, 3886–3892.

[27] Turecek, F.; Brabec, L.; Vondrak, T.; Hanus, V.; Hajicek, J.; Havlas, Z. *Collect. Czech. Chem. Commun.* **1988**, *53*, 2140–2158.

[28] (a) Turecek, F.; Hanus, V. *Org. Mass Spectrom.* **1984**, *19*, 631–638. (b) Iraqi, M.; Pri-Bar, I.; Lifshitz, C. *Org. Mass Spectrom.* **1986**, *21*, 661–671.

[29] Derrick, P. J.; Asbrink, L.; Edquist, O.; Jonsson, B. Ö.; Lindholm, E. *Int. J. Mass Spectrom. Ion Phys.* **1971**, *6*, 203–215.

[30] (a) Maquestiau, A.; Flammang, R.; Pauwels, P. *Org. Mass Spectrom.* **1983**, *18*, 547–552. (b) Traeger, J. C.; Hudson, C. E.; McAdoo, D. J. *Org. Mass Spectrom.* **1988**, *23*, 230–234.

[31] Heats of formation of the products are the following: $\Delta H_f(C_2H_4^{\bullet+} + CO)$ = 957 kJ mol^{-1}; $\Delta H_f(CH_2{=}CHCO^+ + H^{\bullet})$ = 969 kJ mol^{-1}; $\Delta H_f(CH_2{=}C{=}O^{\bullet+} + CH_2)$ = 1270 kJ mol^{-1}; $\Delta H_f({}^+CH{=}C{=}O + CH_3^{\bullet})$ = 1242 kJ mol^{-1}; $\Delta H_f(C_2H_2^{\bullet+} + CH_2O)$ = 1219 kJ mol^{-1}; $\Delta H_f(CH_2O^{\bullet+} + C_2H_2)$ = 1169 kJ mol^{-1}.[32]

[32] Lias, S. G.; Bartmess, J. E.; Liebman, J. F.; Holmes, J. L.; Levin, R. D.; Mallard, W. G. *J. Phys. Chem. Ref. Data* **1988**, *17*, Suppl. 1.

[33] The intensity of the $CH_2{=}C{=}O^{\bullet+}$ ion at m/z 42 was corrected for the contribution of ${}^+CD{=}C{=}O$. The relative intensity of the latter ion was taken to be equal to that of ${}^+CH{=}C{=}O$ in the CAD spectrum of $\mathbf{1a}^{\bullet+}$.

[34] Bouma, W. J.; Gill, P. M. W.; Radom, L. *Org. Mass Spectrom.* **1984**, *19*, 610–616.

[35] Todd, P. J.; McLafferty, F. W. *Int. J. Mass Spectrom. Ion Phys.* **1981**, *38*, 371–379.

[36] This value is probably slightly increased by isobaric overlap with C_2DO^+ at m/z 42 at high precursor ion transmittance. The metastable ion spectrum of $\mathbf{1a}^{\bullet+}$ shows weak peaks of C_2HO^+ and C_2DO^+.

Scheme V

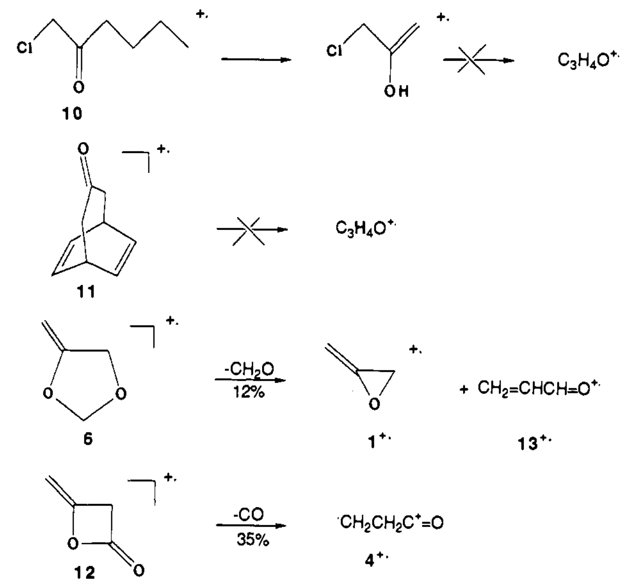

suggests that the CH_2/CD_2 exchange becomes competitive in dissociating $\mathbf{1a}^{\bullet+}$ of an internal energy close to the threshold of the $CH_2{=}C{=}O^{\bullet+} + CH_2$ formation. These effects indicate that the degenerate isomerization in $\mathbf{1}^{\bullet+}$ has a substantial energy barrier that makes it insensitive to collisional activation in nondissociating ions. However, the critical energy of the isomerization is lower than that of the loss of the ring CH_2, which is competitive at higher excitation energies because of its looser transition state.

In contrast to the preparation of $\mathbf{1}^{\bullet+}$, our attempts at generating the cyclopropanone ion $\mathbf{2}^{\bullet+}$ were unsuccessful. Since neutral cyclopropanone is extremely unstable and difficult to handle,[8] we resorted to using its hemiacetal derivative, 1-acetoxycyclopropanol (**8**), which has been employed as a cyclopropanone substitute in solution chemistry.[7d,37] Upon ionization compound **8** afforded $C_3H_4O^{\bullet+}$ in low yield (3%); however, the CAD spectrum of the latter was identical with that of $CH_3CH{=}C{=}O^{\bullet+}$ ($\mathbf{9}^{\bullet+}$), generated from 2,2,5-trimethyl-1,3-dioxane-4,6-dione[30] (Figure 1d). The cyclopropane ring in $\mathbf{8}^{\bullet+}$ apparently opens prior to acetic acid elimination[38] which then proceeds to give rise to the most stable[39] ion $\mathbf{9}^{\bullet+}$ (Scheme IV).

We have also made several attempts at preparing the oxyallyl cation radical $\mathbf{3}^{\bullet+}$ (Scheme V). 1-Chlorohexan-2-one (**10**) and bicyclo[3.2.2]nona-6,8-diene-3-one[40] (**11**) do not give $C_3H_4O^{\bullet+}$ in practically usable yields (>1%), although a complementary C_3H_4O neutral is formed from $\mathbf{11}^{\bullet+}$ dissociating to $C_6H_6^{\bullet+}$ in the ion source.[40] Electron ionization of other logical precursors, 4-methylene-1,3-dioxolane (**6**) and diketene (**12**), yields $C_3H_4O^{\bullet+}$ in 12% and 35% relative abundance (Scheme V). The CAD spectra of these products differ from each other and from that of $\mathbf{1}^{\bullet+}$ in the relative intensities of fragments at *m/z* 55, 42, 41, 30, 29, and 28 (Figure 2). However, the CAD spectrum of $C_3H_4O^{\bullet+}$ from **6** (Figure 2a) can be composed of those of $\mathbf{1}^{\bullet+}$ and $CH_2{=}CHCHO^{\bullet+}$ ($\mathbf{13}^{\bullet+}$, Figure 1e), while the CAD spectrum of $C_3H_4O^{\bullet+}$ from **12** (Figure 2b) is closely similar to that of the stable $^{\bullet}CH_2CH_2CO^+$ distonic ion[41] $\mathbf{4}^{\bullet+}$ generated from succinic anhydride[30b] (Figure 1c), as is also corroborated by its $^+NR^+$ spectrum (below). The formation of $\mathbf{4}^{\bullet+}$ and **12** necessitates a skeletal rearrangement forming the carbon–carbon bond that links the methylene groups; ions $\mathbf{3}^{\bullet+}$ and/or $\mathbf{2}^{\bullet+}$ are possible intermediates in this formation. On collisional charge inversion, the oxyallyl ion $\mathbf{3}^{\bullet+}$ may be expected to yield a stable anion radical depicted as mesomeric enolate forms $\mathbf{3a}^{\bullet-} \leftrightarrow \mathbf{3b}^{\bullet-}$. Formation of stable anions has been shown earlier to be a sensitive probe for the presence of oxygen-centered radicals.[17,42] However, the charge

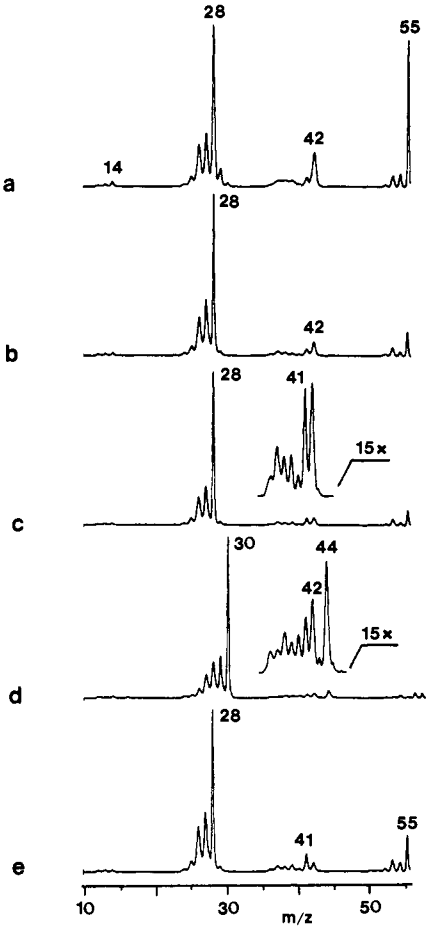

Figure 2. Collisionally activated dissociation spectra (O_2, 50% transmittance) of $C_3H_4O^{\bullet+}$ from (a) **6**, (b) **12**, (c) 4-butanolide, (d) $C_3H_2D_2O^{\bullet+}$ from 4-butanolide-*2,2,4,4-d*$_2$, and (e) $C_3H_4O^{\bullet+}$ from cyclohexane-1,4-dione.

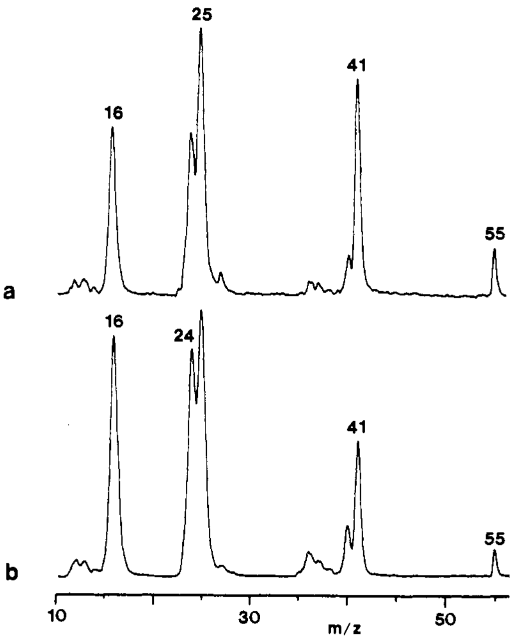

Figure 3. Charge inversion spectra (benzene, 25% transmittance) of $C_3H_4O^{\bullet+}$ from (a) **6** and (b) **12**.

---

(37) van Tilborg, W. J. M.; Steinberg, H.; de Boer, T. J. *Synth. Commun.* **1973**, *3*, 189–196.

(38) For a review on cyclopropane ring opening in gaseous ions see: Schwartz, H. In *The Chemistry of the Cyclopropyl Group*; Rappoport, Z., Ed.; Wiley: Chichester, 1987; Chapter 4, pp 173–211.

(39) Bouchoux, G. *J. Mol. Struct.* (*THEOCHEM*) **1987**, *151*, 107–111.

(40) Hill, A. E.; Hoffman, H. M. R. *J. Am. Chem. Soc.* **1974**, *96*, 4597–4603.

(41) For definition of distonic ions see: Yates, B. F.; Bouma, W. J.; Radom, L. *J. Am. Chem. Soc.* **1984**, *106*, 5805–5808. Review: Hammerum, S. *Mass Spectrom. Rev.* **1988**, *7*, 123–202.

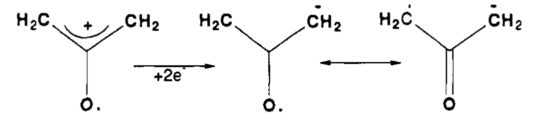

$3^{+\cdot}$ $3a^{-\cdot}$ $3b^{-\cdot}$

inversion spectra of $C_3H_4O^{\bullet+}$ from **6** and **12** (Figure 3) show no detectable peaks of surviving $C_3H_4O^{\bullet-}$.

The formation of $4^{\bullet+}$ from other precursors (e.g., 4-butanolide and cyclohexane-1,4-dione) was further examined in the light of the possible formation of the ion–molecule complex, $CH_2{=}CH_2^{\bullet+}\cdots OC$ ($14^{\bullet+}$), which was predicted by ab initio calculations to be a stable species.[39] While both $4^{\bullet+}$ and $14^{\bullet+}$ can be expected to dissociate readily to $C_2H_4^{\bullet+}$ and CO (Figure 1c), they should differ in the extent and mechanism of CH_2 loss. Dissociation of $4^{\bullet+}$ and $14^{\bullet+}$ by direct loss of CH_2 would produce $CH_2{=}C{=}O^{\bullet+}$ and $:C{=}O{-}CH_2^{\bullet+}$, respectively. The latter has been calculated to be 259 kJ mol^{-1} less stable than $CH_2{=}C{=}O^{\bullet+}$,[34] so the loss of CH_2 from $14^{\bullet+}$ should be highly disfavored, or should proceed with rearrangement to form the more stable ketene ion. The CAD spectra of $C_3H_4O^{\bullet+}$ from the above precursors (Figure 2c,e) differ in the relative abundances of $C_2H_2O^{\bullet+}$ (m/z 42) and $C_2HO^{\bullet+}$ (m/z 41), suggesting formations of different ion mixtures. However, the increased relative abundance at m/z 41 can be due to an admixture of the most stable $CH_3CH{=}C{=}O^{\bullet+}$ ion ($9^{\bullet+}$) whose CAD spectrum displays C_2HO^+ (m/z 41) but negligible $C_2H_2O^{\bullet+}$ (Figure 1d). The $[m/z\ 42]/[m/z\ 41]$ abundance ratio for $4^{\bullet+}$ from succinic anhydride was found to depend on the precursor pressure in the ion source, decreasing from $[m/z\ 42]/[m/z\ 41] = 2.4$ at 2×10^{-6} Torr to 0.9 at 1×10^{-5} Torr. This can also be interpreted by isomerization of $4^{\bullet+}$ to the more stable ketene ion $9^{\bullet+}$ by ion–molecule reactions.

The loss of CH_2 was further scrutinized with the $C_3H_2D_2O^{\bullet+}$ ion, presumably $^{\bullet}CH_2CD_2CO^+$, prepared from 4-butanolide-*2,2,4,4-d*$_4$[43] by the clean elimination of CD_2O without hydrogen deuterium exchange; this indicates that the positional integrity of the label is preserved in the product. Its CAD spectrum (Figure 2d) shows a dominant formation of $CD_2{=}C{=}O^{\bullet+}$ due to loss of $CH_2^{\bullet}$, stepwise deconvolution of the $C_3(H,D)_x$ and $C_2(H,D)O$ isobaric overlaps[33] yield 4% $CH_2{=}C{=}O^{\bullet+}$, 9% $CHD{=}C{=}O^{\bullet+}$, and 87% $CD_2{=}C{=}O^{\bullet+}$. This suggests that (i) $^{\bullet}CH_2CD_2CO^+$ but not $[CH_2{=}CD_2\cdots OC]^{\bullet+}$ is formed from 4-butanolide-*2,2,4,4-d*$_4$ and (ii) the ion does not isomerize appreciably to $^{\bullet}CD_2CH_2CO^+$ or symmetrical structures (e.g. *2-d*$_2^{\bullet+}$, Scheme VI) that would allow CD_2 elimination.

Ion Theoretical Calculations. The experimental data can be interpreted with the help of ion relative energies and barriers to their isomerizations as obtained from ab initio calculations. The calculated total energies and 6-31G* zero-point vibrational energies are summarized in Table I, while Table II gives the relative energies. The methyleneoxirane ion ($1^{\bullet+}$) is calculated to be a stable equilibrium structure (Figure 4a). The C=C bond length (shown in Å) is comparable to those calculated for acyclic enol ions,[44] whereas the =C—O bond is slightly shorter. The CH_2—O bond is conspicuously long, suggesting its facile rupture. The oxyallyl ion $3^{\bullet+}$ is also calculated to be an equilibrium structure (Figure 4b), slightly distorted from C_{2v} symmetry. Geometry optimization with the C_{2v} symmetry restriction yielded a structure of a higher HF/6-31G* energy which, however, approached that of the distorted structure (Figure 4b) upon MP4 post-SCF treatment. The asymmetrical distortion in $3^{\bullet+}$ may be an artifact of the SCF geometry optimization.[45] The ion $3^{\bullet+}$ is destabilized

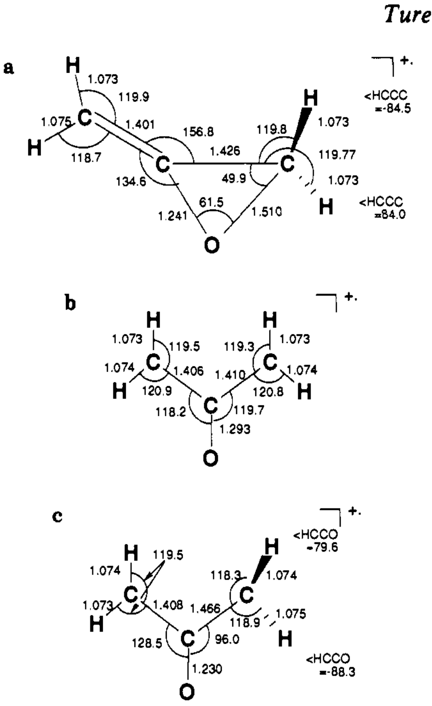

Figure 4. 6-31G* optimized geometries of (a) $1^{\bullet+}$, (b) $3^{\bullet+}$, and (c) TS($1^{\bullet+} \rightarrow 3^{\bullet+}$).

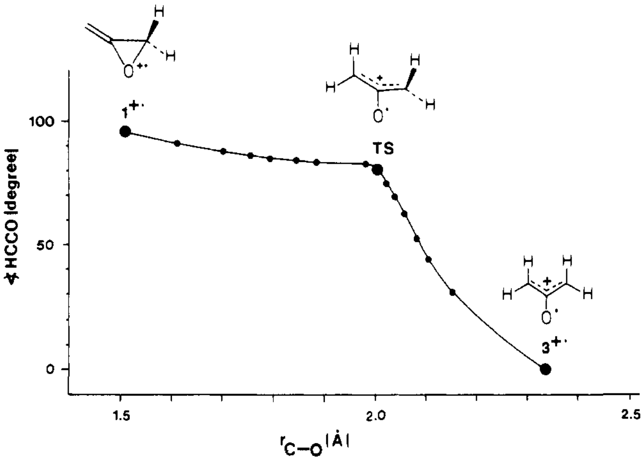

Figure 5. 6-31G* calculated minimum energy reaction path for the $1^{\bullet+} \rightarrow 3^{\bullet+}$ isomerization.

Scheme VI

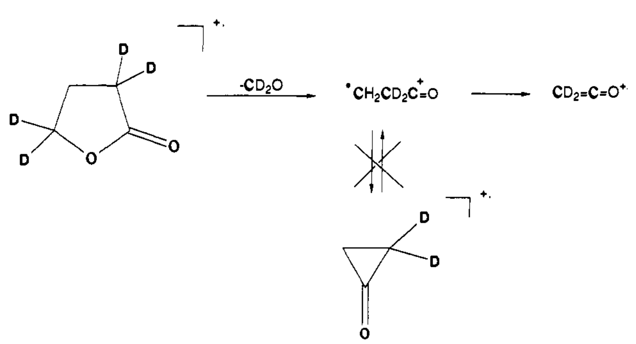

against $1^{\bullet+}$ by 97 kJ mol^{-1}, while the $3^{\bullet+} \rightarrow 1^{\bullet+}$ isomerization requires a very low activation energy (8 kJ mol^{-1}, Table II). This practically precludes specific formation of $3^{\bullet+}$ by dissociative ionization in the gas phase, as the internal energy needed for the exoergic isomerization of $1^{\bullet+}$ can be readily obtained from the thermal energy of the precursor. The reaction path for the $1^{\bullet+} \rightleftarrows 3^{\bullet+}$ isomerization was further investigated by grid calculations, carried out with the 6-31G* basis set, for incremental changes in the CH_2—O bond length and CH_2—C=C torsional angle as

---

(42) (a) Feng, R.; Wesdemiotis, C.; McLafferty, F. W. *J. Am. Chem. Soc.* **1987**, *109*, 6521–6422. (b) Wesdemiotis, C.; McLafferty, F. W. *J. Am. Chem. Soc.* **1987**, *109*, 4760–4761.

(43) McLafferty, F. W.; Barbalas, M. P.; Turecek, F. *J. Am. Chem. Soc.* **1983**, *105*, 1–3.

(44) (a) Bouma, W. J.; MacLeod, J. K.; Radom, L. *J. Am. Chem. Soc.* **1980**, *102*, 2246–2252. (b) Heinrich, N.; Koch, W.; Frenking, G.; Schwarz, H. *J. Am. Chem. Soc.* **1986**, *108*, 593–600. For a review see: Turecek, F. In *The Chemistry of Enols*; Rappoport, Z.; Ed.; Wiley: Chichester, 1990; Chapter 3, pp 96–145.

(45) Davidson, E. R.; Borden, W. T. *J. Phys. Chem.* **1983**, *87*, 4783–4790.

Table I. Calculated Total Ion Energies

species	total energy,[a] hartree				ZPVE,[b] kJ mol^{-1}
	HF	MP2	MP3	MP4	
1$^{\bullet+}$	−190.418 459	−190.938 401	−190.957 551	−190.989 868	154.7
2$^{\bullet+}$	−190.426 864	−190.953 471	−190.971 944	−191.006 344	149.4[c]
3$^{\bullet+}$	−190.413 386	−190.893 558	−190.925 223	−190.952 502	153
4$^{\bullet+}$	−190.467 459	−190.981 744	−190.997 930	−191.032 568	149.4
7$^{\bullet+}$	−190.393 235	−190.883 721	−190.909 261	−190.940 044	150.8
13$^{\bullet+}$	−190.454 620	−190.942 207	−190.972 376	−191.001 801	154.3
14$^{\bullet+}$	−190.457 269	−190.941 638	−190.967 522	−190.998 223	139.9
TS (**1**$^{\bullet+}$→**3**$^{\bullet+}$)	−190.400 992	−190.884 655	−190.914 100	−190.945 209	142.0[c]
$C_2H_4^{\bullet+}$	−77.712 332	−77.917 170	−77.943 124	−77.951 658	125.6
CO	−112.737 877	−113.018 034	−113.017 322	−113.039 241	13.1
$CH_2{=}C{=}O^{\bullet+}$	−151.425 157	−151.810 512	−151.817 786	−151.845 782	87.3[d]
$CH_2(^1A_1)$	−38.811 908	−38.908 812	−38.924 977	−38.929 428	45.9

[a] 1 hartree = 2625.5 kJ mol^{-1}. [b] 6-31G* calculations, scaled by 0.9. [c] Saddle point. [d] From ref 34.

Table II. Relative Ion Energies[a]

ion	rel energy	$\Delta H_f°_{298}$(exp)	$\Delta H_f°_{298}$(calc)[b]
1$^{\bullet+}$	117.4		931
2$^{\bullet+}$	68.9		
3$^{\bullet+}$	213.8		1028
TS (**1**$^{\bullet+}$→**3**$^{\bullet+}$)	222.0		
4$^{\bullet+}$	0.0	816[c]	
7$^{\bullet+}$	244.3		1060
13$^{\bullet+}$	85.6	898[d]	900
14$^{\bullet+}$	79.6		895
$C_2H_4^{\bullet+}$ + CO	98.7	956[d]	919
$C_2H_2O^{\bullet+}$ + $CH_2(^1A_1)$	645.5	1270[d]	

[a] kJ mol^{-1}; MP4/6-31G*/6-31G* + 6-31G* ZPVE scaled by 0.9. [b] Corrected for the heat contents at 298 K with use of the calculated harmonic frequencies and referred to the experimental $\Delta H_f°_{298}$(**4**$^{\bullet+}$).[30b] [c] Reference 30b. [d] Reference 32.

reaction coordinates (Figure 5). The calculated minimum energy path shows that the ring opening in **1**$^{\bullet+}$ is asynchronous with respect to these two reaction coordinates. The reaction begins with stretching the CH_2–O bond up to the saddle point in which the endocyclic CH_2 group is kept almost perpendicular to the ring plane (Figure 4c). In the subsequent potential energy descending phase, the ring opening is nearly synchronous in that it involves continuous changes along both reaction coordinates. It should be noted that, at the 6-31G* level, the local energy minimum pertinent to **3**$^{\bullet+}$ is very shallow with respect to the out-of-plane rotation of either methylene group; for instance, rotation of one methylene by 40° increases the energy by only 1.2 kJ mol^{-1}. This allows for a variety of closely spaced reaction paths as the system is reaching structure **3**$^{\bullet+}$. A similar asynchronicity has been calculated recently for the ring opening in the cyclopropyl radical.[46]

The alternative ring opening in **1**$^{\bullet+}$ by cleavage of the C–C bond leads to the distonic isomer **7**$^{\bullet+}$ (Figure 6a), which was calculated to be a stable structure, 127 kJ mol^{-1} above **1**$^{\bullet+}$. Since **7**$^{\bullet+}$ is planar, the ring opening must involve both C–C bond stretching and CH_2 rotation. Despite many attempts we failed to find the saddle point for the **1**$^{\bullet+}$ → **7**$^{\bullet+}$ isomerization because of SCF convergence problems. However, from the potential energy surface mapping it appears that **1**$^{\bullet+}$ and **7**$^{\bullet+}$ are separated by a significant activation barrier, estimated at >70 kJ mol^{-1} above **7**$^{\bullet+}$. The dissociation of **1**$^{\bullet+}$ to $CH_2{=}C{=}O^{\bullet+}$ and $(^1A_1)CH_2$ is highly endoergic, although the calculated energy difference (529 kJ mol^{-1}, Table II) is probably exaggerated by ≈190 kJ mol^{-1} at the present level of theory.

Our search for the transition state of the isomerization of **3**$^{\bullet+}$ to the cyclopropanone ion **2**$^{\bullet+}$ was unsuccessful because of failing SCF convergence. Ion **2**$^{\bullet+}$ is calculated to be a saddle point with the imaginary frequency ($|\nu|$ = 249 cm^{-1}) corresponding to ring opening by rupture of the CH_2–CO bond. Structure **2**$^{\bullet+}$ (Figure 6b) represents a transition state for the degenerate isomerization of the distonic ion **4**$^{\bullet+}$ (Figure 6c). The instability of **2**$^{\bullet+}$ is analogous to that of the cyclobutanone cation radical which was also calculated to undergo spontaneous ring opening by CH_2–CO bond fission.[47] The further dissociation of **4**$^{\bullet+}$ to $C_2H_4^{\bullet+}$ and CO is calculated to require 99 kJ mol^{-1} whereas the corresponding heat of reaction ($\Delta H_r°$) obtained from the experimental $\Delta H_f°_{298}$ is notably higher (140 kJ mol^{-1}, Table II). Although the energy barrier to the degenerate isomerization, **4**$^{\bullet+}$ → **2**$^{\bullet+}$ → **4**$^{\bullet+}$, is 30 kJ mol^{-1} below the calculated dissociation threshold, the isomerization is inefficient on the microsecond time scale, as established by deuterium labeling (see above). This is probably due to a much tighter transition state for the isomerization (**2**$^{\bullet+}$) compared to that for the dissociation.

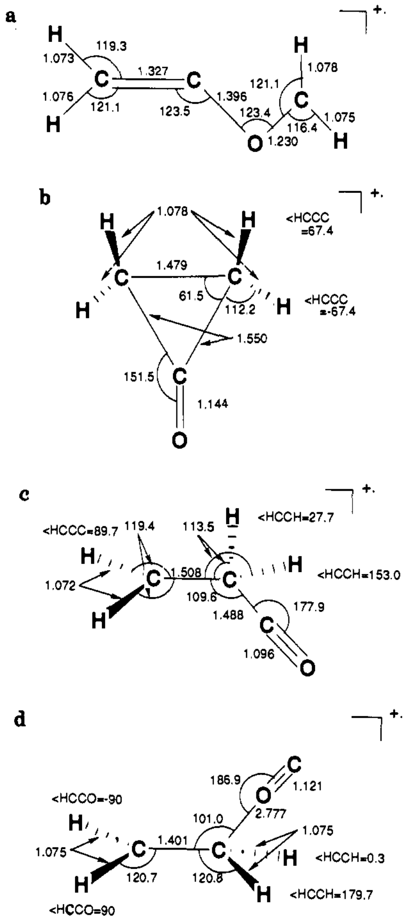

Figure 6. 6-31G* optimized geometries of (a) **7**$^{\bullet+}$, (b) **2**$^{\bullet+}$, (c) **4**$^{\bullet+}$, and (d) **14**$^{\bullet+}$.

The $C_2H_4^{\bullet+}$···OC ion–molecule complex (**14**$^{\bullet+}$, Figure 6d) is calculated to be substantially less stable than **4**$^{\bullet+}$. The dissociation of **14**$^{\bullet+}$ to $C_2H_4^{\bullet+}$ and CO requires only 19 kJ mol^{-1}, so the ion

---

(46) Olivella, S.; Solé, A.; Bofill, J. M. *J. Am. Chem. Soc.* **1990**, *112*, 2160–2167.

(47) Heinrich, N.; Koch, W.; Morrow, J. C.; Schwarz, H. *J. Am. Chem. Soc.* **1988**, *110*, 6332–6336.

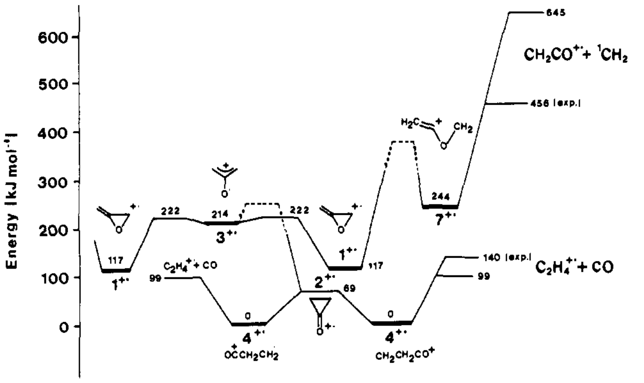

Figure 7. Schematic energy diagram for the isomerization of $C_3H_4O^{•+}$ ions.

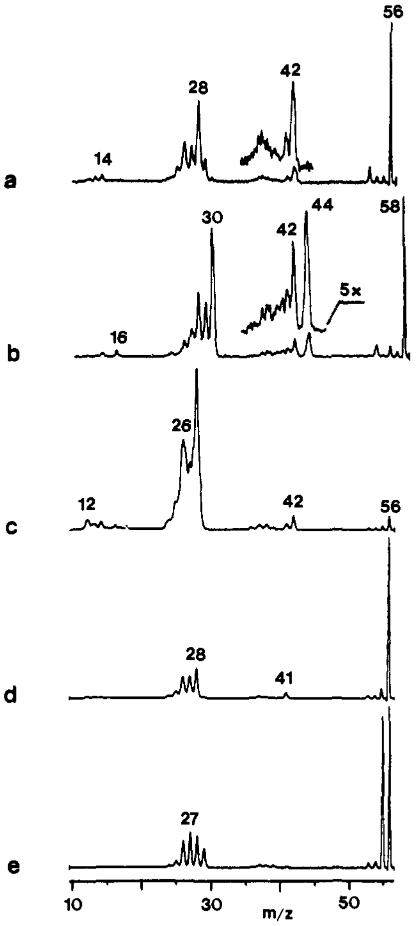

Figure 8. Neutralization-reionization (Hg, 70% transmittance/O_2, 50% transmittance) spectra of (a) $1^{•+}$, (b) $1a^{•+}$, (c) $4^{•+}$, (d) $9^{•+}$, and (e) $13^{•+}$.

is predicted to be only marginally stable. This is consistent with our lack of experimental evidence for the $14^{•+}$ formation. The calculated ion relative energies and isomerization barriers are depicted in a schematic diagram shown in Figure 7. Finally, standard heats of formation ($\Delta H_f{}^{\circ}{}_{298}$), relative to that of $4^{•+}$, were calculated for the stable structures $1^{•+}$, $3^{•+}$, $13^{•+}$, $14^{•+}$, and $C_2H_4{}^{•+}$ and CO with use of the 0 K relative energies and heat contents obtained from scaled harmonic frequencies (Table II).

Neutral Species. Neutralization of $1^{•+}$ yields the stable molecule **1** which following reionization gives a $^+NR^+$ spectrum that shows an abundant survival ion at *m/z* 56 (Figure 8a). The spectrum further shows fragments at *m/z* 42, 30, 29, and 14 which are characteristic of dissociations of $1^{•+}$. The $^+NR^+$ spectrum of the d_2-derivative $1a^{•+}$ shows losses of CH_2 (*m/z* 44) and CD_2 (*m/z* 42), whereas the loss of CHD is negligible (Figure 8b). The corrected[33] $[C_2H_2O^{•+}]/[C_2D_2O^{•+}]$ abundance ratio (0.27) is higher than that in the CAD spectrum of $1a^{•+}$ (0.15, see above), suggesting partial isomerization in the neutral molecules ($1a \rightleftarrows 1b$) or after their reionization ($1a^{•+} \rightleftarrows 1b^{•+}$). The increased relative intensity at *m/z* 28 is in part due to reionization of CO from CAD of $1a^{•+}$. Collisional activation of neutral **1** (He, 50% transmittance) decreases the survival ion abundance (Figure 9a), while increasing the relative intensities of $C_2H_4{}^{•+}$ (*m/z* 28) and $C_2H_2{}^{•+}$ (*m/z* 26). These fragments are also prominent in the $^+NR^+$ spectrum of $^•CH_2CH_2CO^•$ formed by neutralization of $4^{•+}$ (Figure 8c). It is conceivable that upon collisional activation a fraction **1** undergoes the oxyallyl rearrangement to **2**, which subsequently dissociates to C_2H_4 and CO.

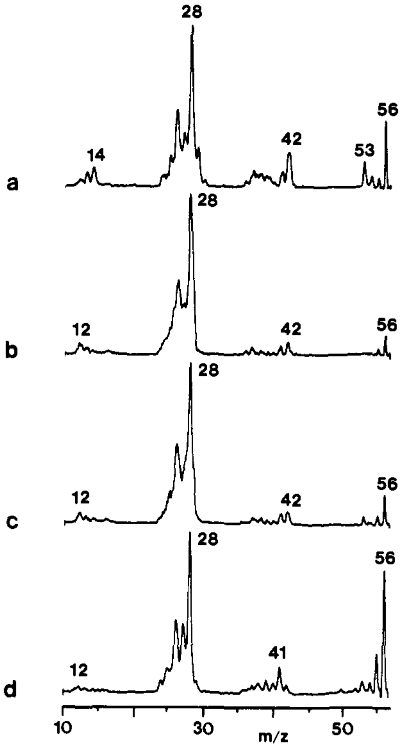

Figure 9. Neutralization-collisional activation-reionization (Hg, 70% transmittance/He, 50% transmittance/O_2, 50% transmittance) spectra of (a) $1^{•+}$, (b) $4^{•+}$, and $C_3H_4O^{•+}$ from (c) **12** and (d) 4-butanolide.

The $^+NR^+$ spectrum of the neutral from $4^{•+}$ shows a very weak survival ion at *m/z* 56 (Figure 8c). The spectrum is dominated by the (C_2H_4 + CO), C_2H_3, and C_2H_2 fragments; the peaks of the latter two are substantially broadened by kinetic energy release. This indicates that the $^•CH_2CH_2CO^•$ biradical (**4**) formed from $4^{•+}$ dissociates exothermically to C_2H_4 and CO which undergo further dissociations (cf. the increased formation of C at *m/z* 12, Figure 8c). The stability of the surviving **4** was further scrutinized by an $^+NCR^+$ experiment (Figure 9b). However, collisional activation did not decrease the relative intensity of the survival $C_3H_4O^{•+}$; this suggests that the latter ion is due to reionization of a stable C_3H_4O isomer (**9** or **13**), present as an impurity in **4**. Consistent with this, the $^+NCR^+$ spectrum of $9^{•+}$ showed only minor changes in the $[C_3H_4O^{•+}]$ relative abundance compared to that in the $^+NR^+$ spectrum. The absence of a detectable survival peak for $^•CH_2CH_2CO^•$ is consistent with the short (<10 ns) lifetimes of 1,3-biradicals in general.[48] A peculiar feature of the $^+NR^+$ spectrum of $4^{•+}$ is the presence of the $C_2H_2O^{•+}$ fragment whose relative intensity does not decrease upon collisional activation of the intermediate neutrals (cf. Figures 8c and 9b). This should not originate from the singlet $^•CH_2CH_2CO^•$ biradical, which should dissociate on formation to C_2H_4 and CO;[48] also *m/z* 42 does not originate from **9** or **13** (Figure 8, d and e). By contrast, the dissociation to C_2H_4 and CO of triplet $^•CH_2CH_2CO^•$ is symmetry forbidden, while $CH_2{=}C{=}O$ and $(^3B_2)CH_2$ can be formed without spin symmetry restrictions. This may in part

---

[48] (a) Johnston, L. J.; Scaiano, J. C. *Chem. Rev.* **1989**, *89*, 521–547. (b) Adam, W.; Grabowski, S.; Wilson, R. M. *Acc. Chem. Res.* **1990**, *23*, 165–172.

Table III. Calculated Total Energies of C_3H_4O Neutral Species

species	total energy, hartrees				ZPVE,[a] kJ mol^{-1}
	HF	MP2	MP3	MP4	
1[b]	−190.703 375	−191.258 778	−191.276 965	−191.308 122	157.9
1[c]	−190.683 241	−191.241 705	−191.258 688	−191.291 733	154.7[d]
2	−190.726 169	−191.280 349	−191.296 957	−191.329 235	156.2
$^{\bullet}CH_2CH_2CO^{\bullet}$ (singlet)	−190.619 080	−191.174 356	−191.186 807	−191.226 907	149.4[d]
$^{\bullet}CH_2CH_2CO^{\bullet}$ (triplet)	−190.632 931	−191.134 247	−191.160 309	−191.100 665	149.4[d]
13	−190.762 424	−191.308 462	−191.327 432	−191.359 575	157.1
$CH_2{=}CH_2{\cdots}OC$[c]	−190.755 721	−191.297 379	−191.315 703	−191.353 939	139.9[d]
$C_2H_4 + CO$	−190.769 595	−191.302 375	−191.322 679	−191.357 937	142.6

[a] 6-31G* calculations. [b] Optimized neutral structure. [c] Structure from vertical neutralization of the cation radical. [d] Assumed to be the same as in the ion.

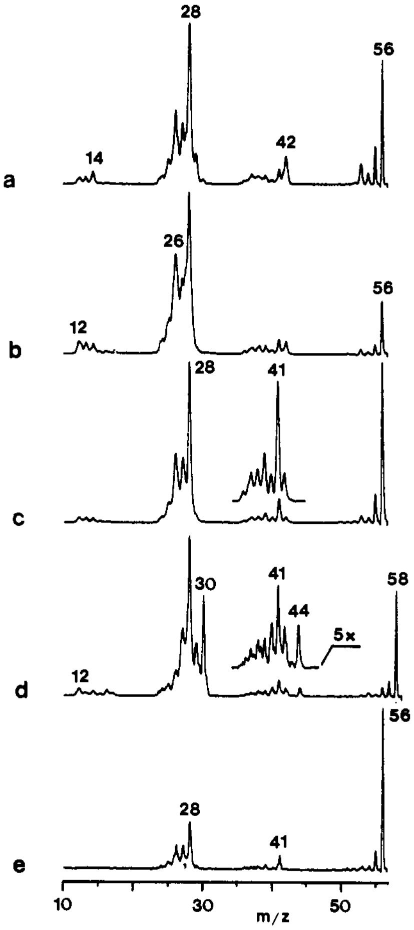

Figure 10. Neutralization-reionization (Hg, 70% transmittance/O_2, 50% transmittance) spectra of $C_3H_4O^{\bullet+}$ from (a) **6**, (b), **12**, (c) 4-butanolide, (d) $C_3H_2D_2O^{\bullet+}$ from 4-butanolide-*2,2,4,4-d₂*, and (e) $C_3H_4O^{\bullet+}$ from cyclohexane-1,4-dione.

balance the large difference in the threshold energies for the dissociations to C_2H_4 and CH_2CO.[49]

The $^+NR^+$ spectrum of $^{\bullet}CH_2CD_2CO^+$ from 4-butanolide-*2,2,4,4-d₄* (Figure 10d) shows preferential loss of CH_2 (*m/z* 44), consistent with the CAD spectrum. The quantitative evaluation of the CH_2/CD_2 interchange is hampered by contamination with $CH_2DCD{=}C{=}O^{\bullet+}$, which gives rise to products at *m/z* 41 and 42 (Figure 10c,d).

The C_3H_4O isomers can further be distinguished by their neutralization-reionization efficiencies[50] that show large differences. While those for **9**$^{\bullet+}$ and **13**$^{\bullet+}$ are comparable (0.0037 and 0.0025, respectively), those for **1**$^{\bullet+}$ and **4**$^{\bullet+}$ are much lower (0.00067 and 0.00014, respectively). This is to be compared with the NR efficiencies of $C_2H_4{}^{\bullet+}$ (0.0053), $CO^{\bullet+}$ (0.0058), and $CH_2{=}C{=}O^{\bullet+}$ (0.0004). The relatively large NR efficiencies of **9**$^{\bullet+}$ and **13**$^{\bullet+}$ make these isomers easily recognizable as admixtures in other $C_3H_4O^{\bullet+}$ species. For example, the survival peak at *m/z* 56 in the $^+NR^+$ spectrum of **4**$^{\bullet+}$ can be accounted for by 0.4% of **9**$^{\bullet+}$. Admixtures of **9**$^{\bullet+}$ in the $C_3H_4O^{\bullet+}$ from 4-butanolide and cyclohexane-1,4-dione are also clearly distinguishable from the $^+NR^+$ spectra (Figure 10c,e). The $^+NR^+$ spectrum of $C_3H_4O^{\bullet+}$ from **12** (Figure 10b) shows fragments characteristic of **4**$^{\bullet+}$ (*m/z* 26, 28) and **1**$^{\bullet+}$ (*m/z* 42). This is further supported by the $^+NCR^+$ spectrum (Figure 9c), which displays a decreased survival ion and an increased fragment at *m/z* 53, consistent with the behavior of **1**$^{\bullet+}$.

Table IV. Relative Energies of C_3H_4O Neutral Species[a]

species	rel energy	$\Delta H_f{}^\circ{}_{298}$(exp)	$\Delta H_f{}^\circ{}_{298}$(calc)[b]
1[c]	147.8		58
1[d]	187.3		
2	89	16,[e] −6[f]	−1
$^{\bullet}CH_2CH_2CO^{\bullet}$[d] (singlet)	350.9		
$^{\bullet}CH_2CH_2CO^{\bullet}$[d] (triplet)	682.3		
13	11.8	−77	
$C_2H_4{\cdots}OC$[d]	10.5		
$C_2H_4 + CO$	0	−58.3[g]	−83

[a] kJ mol^{-1}; MP4/6-31G*/6-31G* + 6-31G* ZPVE scaled by 0.9. [b] Corrected for the heat contents at 298 K with use of the calculated harmonic frequencies and referred to the experimental $\Delta H_f{}^\circ{}_{298}$(**13**).[32] [c] Optimized neutral geometry. [d] Structure from vertical neutralization of the corresponding cation radical. [e] Reference 8. [f] Reference 4. [g] Reference 32.

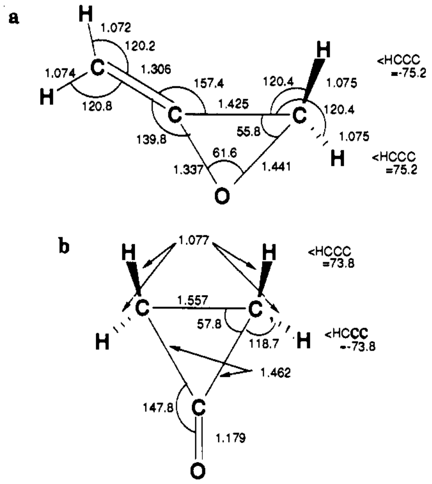

Figure 11. Optimized geometries of (a) **1** and (b) **2**.

Neutral Theoretical Calculations. The relative stabilities of neutral C_3H_4O were assessed by ab initio calculations carried out for both optimized equilibrium structures and those formed by vertical neutralization of the corresponding ions. The calculated total energies and zero-point vibrational corrections are summarized in Table III and the relative energies in Table IV. The calculations show **1** to be a stable equilibrium structure (Figure

---

(49) The pertinent heats of formation are the following: $\Delta H_f(C_2H_4)$ = 52.2 kJ mol^{-1}, $\Delta H_f(CO)$ = −110.5 kJ mol^{-1}, $\Delta H_f(CH_2)$ = 390 kJ mol^{-1}, $\Delta H_f(CH_2{=}C{=}O)$ = −48 kJ mol^{-1}.[32]

(50) These are defined as the ratio of the sum of ion intensities after reionization ($\sum[F_i]$) and the intensity of the incident (unattenuated) precursor ion beam $[M^{\bullet+}]$.

5958 J. Am. Chem. Soc. 1991, 113, 5958–5964

11a) that is metastable with respect to dissociation to C_2H_4 and CO. Vertical neutralization of **1**$^{\bullet+}$ forms a vibrationally excited **1** of ca. 40 kJ mol^{-1} internal energy. According to previous ab initio calculations[3b] such excitation alone is insufficient to bring about isomerization to **2**, consistent with our neutralization–reionization experiments. Cyclopropanone **2** is calculated to be an equilibrium structure (Figure 11b), metastable with respect to dissociation to C_2H_4 and CO, but more stable than **1**. The standard heat of formation of **2** (Table IV), calculated relative to **13** including the 0 K relative energies and 298 K heat contents, is in reasonable agreement with the previous measurements[8] and estimates.[4]

The calculations further predict that the $^{\bullet}CH_2CH_2CO^{\bullet}$ biradical produced by neutralization of **4**$^{\bullet+}$ should be a high-energy species. Dissociation of the $^{\bullet}CH_2CH_2CO^{\bullet}$ singlet to C_2H_4 and CO is predicted to be highly exothermic, consistent with the observed instability of the neutral **4** and the further dissociations of the primary C_2H_4 and CO fragments. The calculated large energy difference between the neutralized singlet and triplet states reflects the different extent of vibrational perturbation upon vertical neutralization rather than the actual singlet–triplet gap in relaxed $^{\bullet}CH_2CH_2CO^{\bullet}$ biradicals.[51] Interestingly, the energy of the $^{\bullet}CH_2CH_2CO^{\bullet}$ triplet is above the threshold for the $CH_2{=}C{=}O$ and CH_2 formation (400 kJ mol^{-1} above C_2H_4 + CO). This may explain the observed competition between these two dissociation channels in a fraction of neutralized **4**. In contrast to **4**, neutralization of **14**$^{\bullet+}$ produces an unbound $C_2H_4 \cdots OC$ complex, which dissociates without barrier to its components. Due to the calculated low exothermicity (10.5 kJ mol^{-1}) for the latter reaction, it should not show a large kinetic energy release as was observed for the dissociations of **4**.

Conclusions

The experimental and theoretical studies demonstrate that methyleneoxirane (**1**$^{\bullet+}$) and $^{\bullet}CH_2CH_2CO^+$ (**4**$^{\bullet+}$) cation radicals are stable species that undergo only limited degenerate isomerizations on collisional activation. The cyclopropanone ion, **2**$^{\bullet+}$, is unstable and functions as a transition state for the degenerate isomerization of **4**$^{\bullet+}$. The oxyallyl cation radical (**3**$^{\bullet+}$) is only marginally stable, and appears as an intermediate in the degenerate isomerization of **1**$^{\bullet+}$ and in the dissociative ionization of diketene (**12**). The neutral molecules **1** and **2** are stable species. Neutralization of **4**$^{\bullet+}$ yields $^{\bullet}CH_2CH_2CO^{\bullet}$ biradicals that decompose within 1 μs. The singlet state is assumed to collapse to C_2H_4 and CO, while the triplet forms $CH_2{=}C{=}O$ and ($^3B_2$)CH_2 in a competing dissociation.

Acknowledgment. We gratefully acknowledge the generous financial support of the National Science Foundation (Grant CHE-8712039) and, for partial instrument funding, the National Institutes of Health (GM16609) and the computational support and technical assistance of the Cornell National Supercomputer Facility, which receives major funding from the National Science Foundation and the IBM corporation, with additional support from New York State and the Corporate Research Institute.

Supplementary Material Available: Table of calculated harmonic vibrational frequencies (2 pages). Ordering information is given on any current masthead page.

---

(51) Borden, W. T.; Ed. *Diradicals*; Wiley-Interscience: New York, 1982.

Gas-Phase Formation and Rearrangements of Methyloxirene and Its Cation Radical

Frantisek Turecek,*,† Donald E. Drinkwater, and Fred W. McLafferty*

Contribution from the Department of Chemistry, Baker Laboratory, Cornell University, Ithaca, New York 14853-1301. *Received December 10, 1990*

Abstract: The gas-phase loss of N_2 from ionized diazoacetone generates the methyloxirene cation radical (**1**$^{\bullet+}$), not ionized methylformylcarbene (**2**$^{\bullet+}$) or acetylcarbene (**3**$^{\bullet+}$), as determined by collisionally activated dissociation (CAD) and charge-inversion mass spectra and isotopic labeling. Vertical neutralization of **1**$^{\bullet+}$ by charge exchange with mercury atoms produces neutral methyloxirene (**1**) that is unstable, rearranging mainly to methylketene and 2-propenal or 1-hydroxypropyne via **2**. This mechanism supports that of Zeller for the corresponding solution photochemistry of the Wolff rearrangement, in contrast to that proposed for the gaseous photochemistry. Semiempirical AM1 and ab initio (MP4/6-31G*//3-21G) calculations predict **1**, **2**, and **3** to exist in potential energy minima separated by low isomerization barriers.

Simple oxirenes represent a class of highly strained antiaromatic heterocycles whose high reactivity has made isolation or direct detection difficult.[1] Methyloxirene (**1**) has been proposed as the key intermediate in the Wolff rearrangement[2] of 2-diazopropanal[3] and diazoacetone,[3,4] interconnecting methylformylcarbene (**2**) and acetylcarbene (**3**), which competitively rearrange to methylketene (**4**, Scheme I, routes d and e). On the basis of ^{13}C label distribution in chemically trapped **4** produced by solution photolysis of [1-^{13}C]-diazoacetone and [1-^{13}C]-2-diazopropanal, Zeller[3] concluded that hydrogen migration, route e, is predominant in **4** formation. In contrast, the gas-phase photolysis of 2-^{13}C-diazoacetone to yield mostly ^{13}CO was interpreted to occur by predominant **3** → **4** methyl migration, route d.[4] Dimethyloxirene (for which routes d and e are identical) has been identified as a minor product of the photolysis of $CH_3COCN_2CH_3$ at 25 K in a rare gas matrix, isomerizing with an activation energy of ~8 kJ mol^{-1} to $O{=}C{=}C(CH_3)_2$ (more abundant) and $CH_2{=}CHCOCH_3$ (homologues of **4** and **5**).[5] Other conceivable pathways, not considered in the previous studies,[3,4] include methyl migration to oxygen in

---

† Present address: Department of Chemistry, University of Washington, Seattle, WA 98195.

(1) For a review on oxirenes see: Lewars, E. G. *Chem. Rev.* **1983**, *83*, 519–534.

(2) Wolff, L. *Liebigs Ann. Chem.* **1902**, *325*, 129.

(3) Zeller, K.-P. *Liebigs Ann. Chem.* **1979**, 2036–2042.

(4) Fenwick, J.; Fater, G.; Ogi, K.; Strausz, O. P. *J. Am. Chem. Soc.* **1973**, *95*, 124–132.

(5) (a) Debu, F.; Monnier, M.; Verlaque, P.; Davidovics, G.; Pourcin, J.; Bodot, H.; Aycard, J.-P. *C.R. Acad. Sci. Paris, Ser. 2* **1986**, *303*, 897–902. (b) Bachmann, C.; N'Guessan, T. Y.; Debu, F.; Monnier, M.; Pourcin, J.; Aycard, J.-P.; Bodot, H. *J. Am. Chem. Soc.* **1990**, *112*, 7488–7497.

0002-7863/91/1513-5958$02.50/0